Journal of Engineering Mathematics **29:** 517–535, 1995.

Modelling the creep of a pipe weld using Cosserat theory

T. D. HAWKES[1] and R. E. CRAINE[2]
[1] *National Economic Research Associates, Stratford Place, London W1N 9AF, U.K.*
[2] *Faculty of Mathematical Studies, University of Southampton, Southampton SO17 1BJ, U.K.*

Received 24 May 1994; accepted in revised form 26 January 1995

Abstract. A mathematical model is developed which describes the steady state creep in a welded pipe which is subjected to a constant uniaxial end load and/or uniform internal and external pressure. The model is based on the Cosserat theory of plates and shells and a generalisation of Norton's law. Both asymptotic and analytical solutions are found and the results reveal that bending and thinning of the pipe take place on different length scales.

1. Introduction

The production of high quality welds is extremely important in many sections of industry. In the power generation industry, for instance, the failure of a single butt-weld in a steam pipe can be extremely costly, since the repair or replacement of the joint may require a generating plant to close for a long time. There have been a number of experimental and theoretical investigations of the complex creep processes that occur in weldments, but these processes are not yet sufficiently well understood for weldments to be included in most high temperature engineering design codes.

Most theoretical work has involved finite element models and results for pipe welds have been found, for instance, by Goodall and Walters [1], Walters [2], Coleman *et al.* [3], Hall and Hayhurst [4] and Tu and Sandström [5]. Obtaining accurate finite element solutions for weldments is difficult and time consuming, however, due to the presence of very narrow material regions and stress singularities.

Recent attempts to find a useful mathematical model have centred on an approach, first introduced by Nicol [6], based on the Cosserat theory of plates and shells. The major feature of the Cosserat theory (see Naghdi [7] for a full discussion) is that the three-dimensional deformation of a general plate (or shell) can be modelled exactly by replacing the plate (or shell) by a two dimensional Cosserat surface situated within the body, provided that to every point of this surface is associated both a displacement and an infinite number of extra variables called directors. The full Cosserat theory is extremely complicated and a simpler model, in which only one director is introduced, is much easier to apply. It is expected that this single director model will yield reasonably accurate solutions for thin plates (or shells) but it is hoped that it will also provide useful approximations for thick plates (or shells). It is important to emphasize that the Cosserat theory for plates is more general than classical theories in that it allows the stress component normal to the plate to be non-zero, and it is this additional flexibility that enables the thinning of a plate to be included within a relatively simple Cosserat model.

The single director Cosserat model was used by Nicol [6] to model the creep of a plate, containing a weld, under uniaxial tension and he obtained solutions for the steady state strain

rate for a number of different weld metals and weld widths. Subsequently Nicol and Williams [8] found parametric equations describing how the strain rate varies with material properties at certain key positions within the weldment. More recently an improved model has been developed which includes, just outside the weld metal, both the narrow type IV region and the narrow heat affected zone (HAZ), and numerous numerical results illustrating the effects on the creep strain rate caused by changing the widths and strengths of the type IV, HAZ and weld regions and by varying the creep index are presented in Hawkes [9] and Craine and Hawkes [10]. The time to rupture and the rupture position have also been calculated recently by Newman and Craine ([11] and [12]) and Newman [13], using a Cosserat model based on a generalised Norton's law and a simple Kachanov-Rabotnov damage law.

All the applications of Cosserat theory mentioned above are for plates, but in this paper we investigate the creep of a welded pipe, a problem of considerable practical importance. Attention is restricted to the steady state creep of a long straight pipe of circular cross-section which contains a weld. The pipe consists of two distinct uniform constituents, the parent material and weld metal, joined at interfaces which are normal to the axis of the pipe, and is subjected to a constant uniaxial tensile force at its ends and to uniform internal and external pressures. Additional narrow regions, such as the narrow type IV region and HAZ which occur in ferritic weldments, are omitted since our principal aim here is to demonstrate that the Cosserat model can be successfully applied to pipes.

The relevant coordinate systems for the pipe are introduced in Section 2 and the appropriate generalised strain rates and stresses calculated in Section 3. After introducing a generalised form of Norton's law in Section 4 the set of equations governing the steady state creep of the pipe are derived. In Section 5 both asymptotic and analytical solutions are found, when the creep index is unity, and the results are discussed in Section 6. Some concluding comments are made in Section 7.

2. Introduction of coordinate systems

A brief derivation of equations governing the steady state creep of a pipe under uniaxial tension is given in Sections 2 to 4 for a Cosserat model. Further details can be found in Hawkes [9] and a full description of the general theory has been presented by Naghdi [7].

Consider a straight pipe of circular cross-section which at time $t = 0$ has constant radius and walls of uniform thickness h. Introduce a set of fixed Cartesian axes, referred to an origin O situated on the central axis of the pipe, with the unit vector $\mathbf{k}$ lying along this axis. The reference surface $\mathcal{S}$ of the pipe lies between its inner and outer surfaces and the position vector of some point $\mathbf{r}$ on this surface can be expressed in terms of Cartesian coordinates (x^1, x^2, x^3) by

$$\mathbf{r} = x^1\mathbf{i} + x^2\mathbf{j} + x^3\mathbf{k}. \tag{2.1}$$

Cosserat theory requires the introduction of curvilinear convected coordinates $(\vartheta^1, \vartheta^2, \vartheta^3)$ such that the two-dimensional reference surface $\mathcal{S}$ is defined by $\vartheta^3 = 0$ for all time, and a suitable choice is the material coordinate system based on the surface $\mathcal{S}$. Choose the positive direction of ϑ^3 to be in the direction of the outward facing normal to $\mathcal{S}$ and let us denote ϑ^3 by r. Suppose z $(= \vartheta^2)$ denotes distance measured along the initially straight, but subsequently deformed, generator of $\mathcal{S}$ at some time t and ϑ $(= \vartheta^1)$ is the angle between a radius and the unit vector $\mathbf{i}$. The radius, R, of the reference surface, measured from the axis of the pipe, can be written $R = R(z, t)$ through symmetry.

The Cartesian coordinates of a point on $\mathcal{S}$ are related to the convected coordinates through

$$x^1 = R(z,t)\cos\vartheta, \qquad x^2 = R(z,t)\sin\vartheta, \qquad x^3 = f(z,t), \tag{2.2}$$

and, on using the definition $\mathbf{a}_\alpha = \partial\mathbf{r}/\partial\vartheta^\alpha$ $(\alpha = 1,2)$, it follows from (2.1) and (2.2) that

$$\mathbf{a}_1 = R(-\sin\vartheta\,\mathbf{i} + \cos\vartheta\,\mathbf{j}), \qquad \mathbf{a}_2 = \frac{\partial R}{\partial z}\cos\vartheta\,\mathbf{i} + \frac{\partial R}{\partial z}\sin\vartheta\,\mathbf{j} + \frac{\partial f}{\partial z}\mathbf{k}. \tag{2.3}$$

These two vectors are tangential to the surface $\mathcal{S}$ so $\mathbf{a}_3$, the unit normal to $\mathcal{S}$, is easy to calculate. Moreover, defining

$$\rho(z,t) = \left(\left(\frac{\partial f}{\partial z}\right)^2 + \left(\frac{\partial R}{\partial z}\right)^2\right)^{1/2}, \tag{2.4}$$

it follows immediately from (2.3) that

$$a_{11} = R^2, \qquad a_{22} = \rho^2, \qquad a_{12} = a_{21} = 0, \qquad a = \det(a_{\alpha\beta}) = R^2\rho^2. \tag{2.5}$$

Assuming that

$$R(z,0) = R_0, \qquad f(z,0) = z, \tag{2.6}$$

the values of $a_{\alpha\beta}$ at $t = 0$, denoted by $A_{\alpha\beta}$, satisfy

$$A_{11} = R_0^2, \qquad A_{22} = 1, \qquad A_{12} = A_{21} = 0, \qquad A = R_0^2. \tag{2.7}$$

It is hoped that no confusion is caused through the use in this paper of superscripts to denote both the contravariant components of a tensor, such as x^2, and the power of a variable, for example ρ^2.

After inverting the matrix $(a_{\alpha\beta})$ to find $(a^{\alpha\beta})$ and then using $\mathbf{a}^\alpha = a^{\alpha\beta}\mathbf{a}_\beta$, where summation over 1 and 2 is assumed for any Greek letter repeated as a superscript and a subscript, we obtain

$$\mathbf{a}^1 = R^{-2}\mathbf{a}_1, \qquad \mathbf{a}^2 = \rho^{-2}\mathbf{a}_2. \tag{2.8}$$

The second fundamental form $b_{\alpha\beta}$ and the Christoffel symbols of the second kind $\Gamma^\gamma_{\alpha\beta}$ are defined by

$$b_{\alpha\beta} = b_{\beta\alpha} = \mathbf{a}_3 \cdot \mathbf{a}_{\alpha,\beta}, \qquad \Gamma^\gamma_{\alpha\beta} = \Gamma^\gamma_{\beta\alpha} = \mathbf{a}^\gamma \cdot \mathbf{a}_{\alpha,\beta} \qquad (\alpha,\beta,\gamma = 1,2), \tag{2.9}$$

and with the use of (2.3) we find that

$$b_{11} = -\frac{R}{\rho}\frac{\partial f}{\partial z}, \qquad b_{22} = \frac{1}{\rho}\left(\frac{\partial^2 R}{\partial z^2}\frac{\partial f}{\partial z} - \frac{\partial R}{\partial z}\frac{\partial^2 f}{\partial z^2}\right), \tag{2.10}$$

$$\Gamma^1_{12} = \Gamma^1_{21} = \frac{1}{R}\frac{\partial R}{\partial z}, \quad \Gamma^2_{11} = -\frac{R}{\rho^2}\frac{\partial R}{\partial z}, \quad \Gamma^2_{22} = \frac{1}{\rho^2}\left(\frac{\partial R}{\partial z}\frac{\partial^2 R}{\partial z^2} + \frac{\partial f}{\partial z}\frac{\partial^2 f}{\partial z^2}\right), \tag{2.11}$$

with all other components being zero. Recalling the initial conditions (2.6) it is easily seen from (2.10) and (2.11) that all components of $\Gamma^\alpha_{\beta\gamma}$ are zero at $t = 0$, and that the only non-zero component of $b_{\alpha\beta}$ initially is

$$B_{11} = -R_0. \tag{2.12}$$

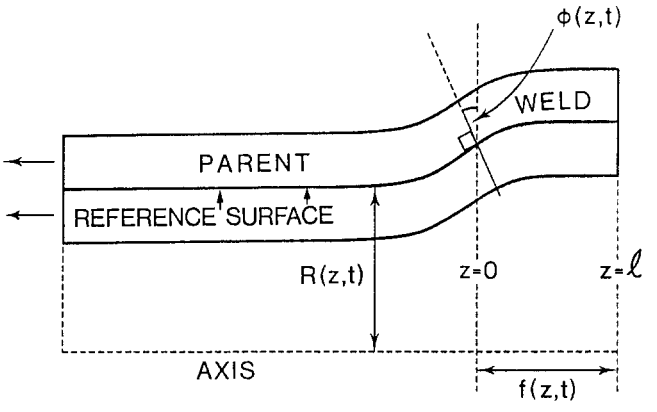

Fig. 1. Section of deformed pipe wall.

Let $\mathbf{p}$ be the position of a general point in the deformed pipe with Cartesian coordinates (y^1, y^2, y^3), so that

$$\mathbf{p} = y^1\mathbf{i} + y^2\mathbf{j} + y^3\mathbf{k}. \tag{2.13}$$

In terms of convected coordinates the inner and outer surfaces of the pipe are given, for all t, by $r = \nu_{\text{in}}$ and $r = \nu_{\text{out}}$ respectively, where ν_{in} and ν_{out} are constants, and hence as the pipe deforms the distance scale in the r-direction must vary with position and time. As a result the expressions relating (y^1, y^2, y^3) to (ϑ, z, r) can be written

$$y^1 = (R + c\cos\phi)\cos\vartheta, \quad y^2 = (R + c\cos\phi)\sin\vartheta, \qquad y^3 = (f - c\sin\phi), \tag{2.14}$$

where $\phi = \phi(z,t)$ is the angle between $\mathbf{a}_3$ and the plane perpendicular to the central axis of the cylinder (see Fig. 1), $c = c(z,r,t)$ is distance in the r-direction and R and f are the functions introduced in (2.2). In an analogous way to the calculation of the base vectors $\mathbf{a}_i$ we can determine from equations (2.13) and (2.14) the covariant base vectors $\mathbf{g}_i$ through use of

$$\mathbf{g}_i = \frac{\partial \mathbf{p}}{\partial \vartheta^i} \qquad (i = 1, 2 \text{ and } 3), \tag{2.15}$$

and go on to obtain the associated reciprocal base vectors $\mathbf{g}^i$ and components G_{ij} and G^{ij} of the metric tensor at $t = 0$. With the additional initial conditions

$$c(z,r,0) = r, \qquad \phi(z,0) = 0, \tag{2.16}$$

it can be shown that the only non-zero initial values of the components of the metric tensor are

$$G_{11} = (G^{11})^{-1} = (R_0 + r)^2, \qquad G_{22} = G^{22} = G_{33} = G^{33} = 1. \tag{2.17}$$

3. Generalised strain rates and stresses

The single director is introduced into our simple Cosserat model through the assumption that $\mathbf{p}$ can be expressed

$$\mathbf{p}(\vartheta, z, r, t) = \mathbf{r}(\vartheta, z, t) + r\,\mathbf{d}(\vartheta, z, t). \tag{3.1}$$

When $\mathbf{d}$ is referred to the base vectors $\mathbf{a}^i$ it can be shown that

$$\frac{\partial \mathbf{d}}{\partial \vartheta^\alpha} = \lambda_{i\alpha}\mathbf{a}^i, \tag{3.2}$$

where

$$\lambda_{\gamma\alpha} = \frac{\partial d_\gamma}{\partial \vartheta^\alpha} - \Gamma^\beta_{\gamma\alpha} d_\beta - b_{\gamma\alpha} d_3, \qquad \lambda_{3\alpha} = \frac{\partial d_3}{\partial \vartheta^\alpha} + b^\gamma_\alpha d_\gamma. \tag{3.3}$$

The kinematic strain variables can now be defined by

$$e_{\alpha\beta} = \frac{1}{2}(a_{\alpha\beta} - A_{\alpha\beta}), \qquad \kappa_{i\alpha} = \lambda_{i\alpha} - \Lambda_{i\alpha}, \qquad \gamma_i = d_i - D_i, \tag{3.4}$$

where D_i and $\Lambda_{i\alpha}$ are the values at $t = 0$ of d_i and $\lambda_{i\alpha}$ respectively. Since our problem is axisymmetric it can be assumed that

$$d_1 = D_1 = 0, \qquad \frac{\partial}{\partial \vartheta} \equiv 0. \tag{3.5}$$

With the aid of equations (2.5) to (2.7), (2.10), (2.11), (2.16) and the simplifications (3.5), the general expressions for the kinematic strain variables (3.4) are then easily calculated.

In an analogous way to previous authors we next assume that throughout the creep regime the deformation of each point of the pipe from its initial position remains small. Thus, we define

$$R = R_0(1 + \varepsilon R_1), \qquad f = z + \varepsilon f_1, \qquad d_i = D_i + \varepsilon \delta_i, \tag{3.6}$$

where the functions R_1, f_1 and δ_i depend on the variables z and t only, ε is a small parameter and terms of $O(\varepsilon^2)$ are neglected. Without loss of generality it is also assumed that

$$\mathbf{D} = (0, 0, 1). \tag{3.7}$$

With the above assumptions it can be shown that

$$\dot{e}_{12} = \dot{e}_{21} = \dot{\kappa}_{12} = \dot{\kappa}_{21} = \dot{\kappa}_{31} = \dot{\gamma}_1 = 0, \tag{3.8}$$

and that the non-zero strain rates, to leading order in ε, are

$$\dot{e}_{11} = \varepsilon R_0^2 \dot{R}_1, \qquad \dot{e}_{22} = \varepsilon \frac{\partial \dot{f}}{\partial z}, \qquad \dot{\kappa}_{11} = \varepsilon R_0(\dot{\delta}_3 + \dot{R}_1), \tag{3.9}$$

$$\dot{\kappa}_{22} = \varepsilon\left(\frac{\partial \dot{\delta}_2}{\partial z} - R_0 \frac{\partial^2 \dot{R}_1}{\partial z^2}\right), \qquad \dot{\kappa}_{23} = \varepsilon \frac{\partial \dot{\delta}_3}{\partial z}, \qquad \dot{\gamma}_2 = \varepsilon \dot{\delta}_2, \qquad \dot{\gamma}_3 = \varepsilon \dot{\delta}_3, \tag{3.10}$$

where throughout this paper a superposed dot denotes differentiation with respect to time t.

Next we must define the generalised two-dimensional Cosserat stress variables in terms of the components σ^{ij} of the usual three-dimensional stress tensor. For our single director model the generalised stresses $\mathbf{N}^\alpha$, $\mathbf{M}^\alpha$ ($\alpha = 1, 2$) and $\mathbf{m}$ must be introduced and, to leading order in ε, the appropriate expressions for the components of these stresses are

$$N^{\alpha i} A^{1/2} = \int_{\nu_{\text{in}}}^{\nu_{\text{out}}} G^{1/2} \sigma^{\alpha j} \mu^i_j \, \mathrm{d}r, \qquad M^{\alpha i} A^{1/2} = \int_{\nu_{\text{in}}}^{\nu_{\text{out}}} G^{1/2} \sigma^{\alpha j} \mu^i_j r \, \mathrm{d}r, \tag{3.11}$$

$$m^i A^{1/2} = \int_{\nu_{\text{in}}}^{\nu_{\text{out}}} G^{1/2}\sigma^{3j}\mu_j^i \, \mathrm{d}r, \tag{3.12}$$

where

$$G = \det(G_{ij}) = (R_0 + r)^2, \qquad \mu_j^i = \mathbf{G}_j \cdot \mathbf{A}^i. \tag{3.13}$$

Expressions for ν_{in} and ν_{out} are found by solving the pair of equations

$$\int_{\nu_{\text{in}}}^{\nu_{\text{out}}} \rho_0 G^{1/2} r \, \mathrm{d}r = 0, \qquad \nu_{\text{out}} - \nu_{\text{in}} = h. \tag{3.14}$$

Condition $(3.14)_1$ controls the distribution of mass about the surface $r = 0$ (see [7] for further discussion). Assuming ρ_0, the initial density of the body, is constant it is easily shown from $(3.13)_1$ and (3.14) that

$$\nu_{\text{in}} = h\left(-\frac{1}{2} - \frac{\tau}{12} - \frac{\tau^3}{144} + \mathrm{O}(\tau^5)\right), \qquad \text{where } \tau = \frac{h}{R_0}. \tag{3.15}$$

In this work it is assumed that $\varepsilon \ll \tau \ll 1$.

To develop the model further it is necessary to obtain expressions for the stress components σ^{ij} in terms of the components $N^{\alpha i}$, $M^{\alpha i}$ and m^i. To this end we assume that

$$\sigma^{\alpha i} = a^{\alpha i} + c^{\alpha i} r, \qquad \sigma^{3i} = a^{3i}, \qquad (\alpha = 1,2; \quad i = 1,2,3), \tag{3.16}$$

where a^{ji} and $c^{\alpha i}$ are constants. More complicated expressions for $\sigma^{\alpha i}$ could be introduced but these would require the appearance in the model of additional generalised stresses and extra directors, and the model then becomes much more involved. With the aid of $(3.13)_1$, $(3.15)_1$ and (3.16), the integrals in (3.11) and (3.12) can be evaluated, retaining the leading order terms in the small parameter τ. Inverting these expressions it follows, to leading order in τ, that

$$a^{11} = \frac{N^{11}}{h} - \frac{M^{11}}{hR_0}, \quad c^{11} = -\frac{N^{11}}{hR_0} + \frac{12M^{11}}{h^3}, \quad a^{22} = \frac{N^{22}}{h}, \quad c^{22} = \frac{12M^{22}}{h^3}, \tag{3.17}$$

$$a^{23} = \frac{N^{23}}{h}, \qquad c^{23} = \frac{12M^{23}}{h^3}, \qquad a^{32} = \frac{m^2}{h}, \qquad a^{33} = \frac{m^3}{h}. \tag{3.18}$$

Substituting the above results into (3.16) provides the necessary approximate expressions for the components of the three-dimensional stress tensor in terms of the corresponding two-dimensional components.

4. Derivation of the governing equations

Above a certain critical temperature metals, under load, exhibit a time-dependent deformation known as creep. The latter is normally divided into three main stages called primary, secondary and tertiary. The secondary creep régime is usually much longer than the other two and is often the only one included in a long term creep model. Within the secondary creep régime all strain rates are approximately constant, and Norton's law is normally used to describe the material behaviour. Hawkes [9] has shown that the appropriate generalisation of Norton's law for the pipe problem being considered here is

$$\dot{\mathbf{\Phi}} = \frac{A}{2N^*}\left[\frac{N^*}{\sigma_c h}\right]^n \frac{\partial N^{*2}}{\partial \mathbf{\Psi}}, \tag{4.1}$$

where $\mathbf{\Phi}$ and $\mathbf{\Psi}$ denote the sets of variables

$$\mathbf{\Phi} = (e_{\alpha\beta}, \kappa_{\alpha\beta}, \kappa_{3\alpha}, \gamma_\alpha, \gamma_3), \qquad \mathbf{\Psi} = (N'^{\alpha\beta}, M^{\alpha\beta}, M^{\alpha 3}, m^\alpha, m^3), \tag{4.2}$$

and a typical stress σ_c, material strength A and creep index n are all constants. Note that, because of invariance requirements, $N^{\alpha\beta}$ has been replaced in $(4.2)_2$ by $N'^{\alpha\beta}$ which is defined by

$$N'^{\alpha\beta} = N'^{\beta\alpha} = N^{\alpha\beta} + M^{\gamma\alpha} b^\beta_\gamma. \tag{4.3}$$

The Von Mises equivalent stress σ^* and stress invariant N^*, which appear in (4.1), are defined by

$$\sigma^{*2} = \frac{3}{2}\left(\sigma^i_j - \frac{1}{3}\delta^i_j\sigma^k_k\right)\left(\sigma^j_i - \frac{1}{3}\delta^j_i\sigma^m_m\right), \qquad N^{*2} = h\int_{\nu_{\text{in}}}^{\nu_{\text{out}}} \sigma^{*2}\,\mathrm{d}r. \tag{4.4}$$

Using the metric tensor g_{ij} it is straightforward to write σ^{*2} in terms of the contravariant components σ^{ij} and, with the aid of (2.12), (2.17), (3.15) to (3.18) and (4.3), it then follows from $(4.4)_2$ that the leading order terms in N^{*2} become

$$\begin{aligned} N^{*2} \;=\; & R_0^4(N'^{11})^2 + 12\frac{R_0^4}{h^2}(M^{11})^2 + (N^{22})^2 - \frac{2}{R_0}N^{22}M^{22} + \frac{12}{h^2}(M^{22})^2 \\ & + (m^3)^2 - R_0^2N'^{11}m^3 - N^{22}m^3 + \frac{1}{R_0}M^{22}m^3 - R_0^2N'^{11}N^{22} - R_0N^{22}M^{11} \\ & - 12\frac{R_0^2}{h^2}M^{11}M^{22} + 3(N^{23})^2 - \frac{6}{R_0}N^{23}M^{23} + \frac{36}{h^2}(M^{23})^2. \end{aligned} \tag{4.5}$$

Define ω by

$$\omega = \frac{A}{2N^*}\left(\frac{N^*}{\sigma_c h}\right)^n, \tag{4.6}$$

then on substituting (4.5) into (4.1) and using equations (3.8) to (3.10) and (4.2) we obtain

$$\varepsilon R_0^2\dot{R}_1 = \omega(2R_0^4N'^{11} - R_0^2N^{22} - R_0^2m^3), \tag{4.7}$$

$$\varepsilon\frac{\mathrm{d}\dot{f}_1}{\mathrm{d}z} = \omega\left(-R_0^2N'^{11} + 2N^{22} - R_0M^{11} - \frac{2}{R_0}M^{22} - m^3\right), \tag{4.8}$$

$$\varepsilon(R_0\dot{\delta}_3 + R_0\dot{R}_1) = \omega\left(-R_0N^{22} + 24\frac{R_0^4}{h^2}M^{11} - 12\frac{R_0^2}{h^2}M^{22}\right), \tag{4.9}$$

$$\varepsilon\left(\frac{\mathrm{d}\dot{\delta}_2}{\mathrm{d}z} - R_0\frac{\mathrm{d}^2\dot{R}_1}{\mathrm{d}z^2}\right) = \omega\left(-\frac{2}{R_0}N^{22} - 12\frac{R_0^2}{h^2}M^{11} + \frac{24}{h^2}M^{22} + \frac{m^3}{R_0}\right), \tag{4.10}$$

$$\varepsilon\dot{\delta}_3 = \omega\left(-R_0^2N'^{11} - N^{22} + \frac{M^{22}}{R_0} + 2m^3\right), \tag{4.11}$$

$$\varepsilon\dot{\delta}_2 = 6\omega\left(N^{23} - \frac{1}{R_0}M^{23}\right), \tag{4.12}$$

$$\varepsilon \frac{\mathrm{d}\dot{\delta}_3}{\mathrm{d}z} = 6\omega \left(-\frac{1}{R_0} N^{23} + \frac{12}{h^2} M^{23} \right). \tag{4.13}$$

In stating equations (4.7) to (4.13) higher order terms in τ and ε have been neglected and, since we are restricting attention to steady state creep, ordinary derivatives with respect to z are now appropriate. It is assumed that the terms appearing in (4.7) to (4.13) balance to $\mathrm{O}(\varepsilon)$ and hence choosing $\varepsilon = 1$, as we shall do in Section 5, is equivalent to a simple rescaling of the stresses.

Since creep in a metal is a very slow time-dependent deformation the inertia terms in the plate equations stated in [7] can be neglected. Hence, for the problem under discussion, the linearized forms of these plate equations become

$$\frac{\mathrm{d}N^{22}}{\mathrm{d}z} = 0, \qquad \frac{\mathrm{d}M^{23}}{\mathrm{d}z} - R_0 M^{11} = m^3 - \rho_0 L^3, \tag{4.14}$$

$$\frac{\mathrm{d}N^{23}}{\mathrm{d}z} = R_0 N^{11} - \rho_0 F^3, \qquad \frac{\mathrm{d}M^{22}}{\mathrm{d}z} = N^{23}, \tag{4.15}$$

where, in the absence of body forces, the contravariant variables L^3 and F^3 depend on the applied pressures. The constant internal and external pressures, p_i and p_e respectively, satisfy

$$\sigma_3^3 = -p_i \text{ on } r = \nu_{\text{in}}, \qquad \sigma_3^3 = -p_e \text{ on } r = \nu_{\text{out}}. \tag{4.16}$$

Then, defining the sum and difference of the pressures by

$$p_s = p_i + p_e, \qquad p_d = p_i - p_e, \tag{4.17}$$

it can be shown that, neglecting terms of $\mathrm{O}(\tau^2)$,

$$\rho_0 L^3 = h \left(-\frac{p_s}{2} + \frac{\tau p_d}{6} \right), \qquad \rho_0 F^3 = p_d - \frac{\tau p_s}{2}. \tag{4.18}$$

Eliminating L^3 and F^3 using equations (4.18), M^{11} by equation (4.9) and N'^{11} and m^3 by equations (4.7) and (4.11), the remaining equations (4.8), (4.10), and (4.12) to (4.15) can be expressed as a set of eight first order differential equations in the stresses

$$N^{22}, \qquad N^{23}, \qquad M^{22}, \qquad M^{23} \tag{4.19}$$

and the associated strain rates

$$\dot{f}_1, \quad \dot{R}_1, \quad \dot{\delta}_2 - R_0 \frac{\mathrm{d}\dot{R}_1}{\mathrm{d}z}, \quad \dot{\delta}_3. \tag{4.20}$$

This set of equations must be solved when the material parameter A and creep index n are constant within the parent material and weld metal separately, but change discontinuously at the interfaces between these regions. Due to symmetry only one half of the pipe need be considered in our solution. From the form of the differential equations it is evident that to complete the system the eight variables (4.19) and (4.20) must all be continuous at the parent-weld interface (i.e. $z = 0$) and, in addition, a total of eight boundary conditions must be applied to these variables at the end of the pipe ($z \to -\infty$) and at the centre of the weld ($z = l$).

At $z = l$ symmetry implies that

$$\frac{\mathrm{d}\dot{R}_1}{\mathrm{d}z} = 0 = \frac{\mathrm{d}\dot{f}_1}{\mathrm{d}z} = \frac{\mathrm{d}\dot{\delta}_3}{\mathrm{d}z}, \qquad \frac{\mathrm{d}N^{22}}{\mathrm{d}z} = 0 = \frac{\mathrm{d}M^{22}}{\mathrm{d}z}. \tag{4.21}$$

Noting from $(4.14)_1$ that condition $(4.21)_4$ is identically satisfied, it is easily seen with the aid of (4.13) and $(4.15)_2$ that the requirements (4.21) are equivalent to

$$\frac{\mathrm{d}\dot{R}_1}{\mathrm{d}z} = 0 = \frac{\mathrm{d}\dot{f}_1}{\mathrm{d}z} = M^{23} = N^{23} \text{ on } z = l. \tag{4.22}$$

As the ends of the pipe are approached the three-dimensional stress components σ_2^2 and σ_3^2 can be specified, and hence

$$N^{22}, M^{22}, N^{23} \text{ and } M^{23} \text{ are known as } z \to -\infty. \tag{4.23}$$

Solutions of the set of equations (4.7) to (4.15) that satisfy conditions (4.22), (4.23) and the continuity of the variables (4.19) and (4.20) at the interface $z = 0$ are found in the following section.

5. Solution of the governing systems of equations

It follows immediately from equation $(4.14)_1$, condition $(4.21)_4$ and the continuity of N^{22} at the parent-weld interface that N^{22} is constant, $= N_\infty$ say, throughout the pipe. Using the latter as a typical stress value we introduce the non-dimensional variables

$$\dot{\bar{R}}_1 = \frac{2\dot{R}_1\sigma_c h}{A_a N_\infty}, \qquad \dot{\bar{e}}_{22} = \frac{2\dot{e}_{22}\sigma_c h}{A_a N_\infty}, \qquad \dot{\bar{\delta}}_2 = \frac{2\dot{\delta}_2\sigma_c R_0}{A_a N_\infty}, \tag{5.1}$$

$$\dot{\bar{\delta}}_3 = \frac{2\dot{\delta}_3\sigma_c h}{A_a N_\infty}, \qquad \bar{N}_1^1 = \frac{R_0^2 N'^{11}}{N_\infty}, \qquad \bar{m}_3 = \frac{m^3}{N_\infty}, \tag{5.2}$$

$$\bar{M}_1^1 = \frac{R_0^3 M^{11}}{h^2 N_\infty}, \qquad \bar{M}_2^2 = \frac{R_0 M^{22}}{h^2 N_\infty}, \qquad \bar{N}_{23} = \frac{R_0 N^{23}}{h N_\infty}, \tag{5.3}$$

$$\bar{M}_{23} = \frac{M^{23}}{h N_\infty}, \qquad \bar{p}_s = \frac{p_s R_0}{N_\infty}, \qquad \bar{p}_d = \frac{p_d R_0}{N_\infty}, \tag{5.4}$$

$$\bar{z} = \frac{z}{R_0}, \qquad \bar{A} = \frac{A}{A_a}, \tag{5.5}$$

where A_a is the constant denoting the strength of the parent material.

For real materials the creep index, n, usually varies between 2 and 10 but in the remainder of this paper we shall assume $n = 1$, the 'elastic case', since this postulate greatly simplifies the analysis and is not expected to change the qualitative features of the solution. Using (5.1) to (5.5) and $n = 1$, it is straightforward to show that equations (4.7) to (4.13) (with $\varepsilon = 1$), $(4.14)_2$ and (4.15) reduce to

$$\dot{\bar{R}}_1 = \bar{A}(2\bar{N}_1^1 - 1 - \bar{m}_3), \qquad \dot{\bar{e}}_{22} = \bar{A}(-\bar{N}_1^1 + 2 - \bar{m}_3), \tag{5.6}$$

$$\dot{\bar{\delta}}_3 + \dot{\bar{R}}_1 = \bar{A}(-1 + 24\bar{M}_1^1 - 12\bar{M}_2^2), \tag{5.7}$$

$$\tau\frac{\mathrm{d}\dot{\bar{\delta}}_2}{\mathrm{d}\bar{z}} - \frac{\mathrm{d}^2\dot{\bar{R}}_1}{\mathrm{d}\bar{z}^2} = \bar{A}(-2 - 12\bar{M}_1^1 + 24\bar{M}_2^2 + \bar{m}_3), \tag{5.8}$$

$$\dot{\bar{\delta}}_3 = \bar{A}(-\bar{N}_1^1 - 1 + 2\bar{m}_3), \qquad \dot{\bar{\delta}}_2 = 6\bar{A}(\bar{N}_{23} - \bar{M}_{23}), \tag{5.9}$$

$$\tau\frac{\mathrm{d}\dot{\bar{\delta}}_3}{\mathrm{d}\bar{z}} = 72\bar{A}\bar{M}_{23}, \qquad \tau\frac{\mathrm{d}\bar{M}_{23}}{\mathrm{d}\bar{z}} = \bar{m}_3 + \frac{1}{2}\tau\bar{p}_s, \tag{5.10}$$

$$\tau\frac{\mathrm{d}\bar{N}_{23}}{\mathrm{d}\bar{z}} = \bar{N}_1^1 - \bar{p}_d + \frac{1}{2}\tau\bar{p}_s, \qquad \tau\frac{\mathrm{d}\bar{M}_2^2}{\mathrm{d}\bar{z}} = \bar{N}_{23}. \tag{5.11}$$

Equations $(5.6)_1$, (5.7) and $(5.9)_{1,2}$ combine to give the four algebraic equations

$$\bar{N}_1^1 = \frac{1}{3\bar{A}}(3\bar{A} + 2\dot{\bar{R}}_1 + \dot{\bar{\delta}}_3), \qquad \bar{M}_1^1 = \frac{1}{24\bar{A}}(\dot{\bar{R}}_1 + \dot{\bar{\delta}}_3 + \bar{A}) + \frac{1}{2}\bar{M}_2^2, \tag{5.12}$$

$$\bar{m}_3 = \frac{1}{3\bar{A}}(3\bar{A} + \dot{\bar{R}}_1 + 2\dot{\bar{\delta}}_3), \qquad \dot{\bar{\delta}}_2 = 6\bar{A}(\bar{N}_{23} - \bar{M}_{23}). \tag{5.13}$$

On defining a new variable $\dot{\bar{S}}$ through

$$\dot{\bar{S}} = \tau\dot{\bar{\delta}}_2 - \frac{\mathrm{d}\dot{\bar{R}}_1}{\mathrm{d}\bar{z}}, \tag{5.14}$$

and with the aid of equations (5.12) and (5.13), the second order differential equation (5.8) can be replaced by the pair of first order equations

$$\frac{\mathrm{d}\dot{\bar{S}}}{\mathrm{d}\bar{z}} = \bar{A}\left(-\frac{3}{2} + 18\bar{M}_2^2\right) - \frac{1}{6}\dot{\bar{R}}_1 + \frac{1}{6}\dot{\bar{\delta}}_3, \tag{5.15}$$

$$\frac{\mathrm{d}\dot{\bar{R}}_1}{\mathrm{d}\bar{z}} = 6\tau\bar{A}(\bar{N}_{23} - \bar{M}_{23}) - \dot{\bar{S}}. \tag{5.16}$$

Moreover, using (5.12) and (5.13) equations (5.10) and (5.11) become

$$\tau\frac{\mathrm{d}\dot{\bar{\delta}}_3}{\mathrm{d}\bar{z}} = 72\bar{A}\bar{M}_{23}, \qquad \tau\frac{\mathrm{d}\bar{M}_{23}}{\mathrm{d}\bar{z}} = \frac{1}{3\bar{A}}(3\bar{A} + \dot{\bar{R}}_1 + 2\dot{\bar{\delta}}_3) + \frac{1}{2}\tau\bar{p}_s, \tag{5.17}$$

$$\tau\frac{\mathrm{d}\bar{N}_{23}}{\mathrm{d}\bar{z}} = \frac{1}{3\bar{A}}(3\bar{A} + 2\dot{\bar{R}}_1 + \dot{\bar{\delta}}_3) - \bar{p}_d + \frac{1}{2}\tau\bar{p}_s, \qquad \tau\frac{\mathrm{d}\bar{M}_2^2}{\mathrm{d}\bar{z}} = \bar{N}_{23}. \tag{5.18}$$

When known pressures are applied to the pipe equations (5.15) to (5.18) form a system of six first order ordinary differential equations for the variables $\dot{\bar{S}}$, $\dot{\bar{R}}_1$, $\dot{\bar{\delta}}_3$, $\bar{M}_{23}$, $\bar{N}_{23}$ and $\bar{M}_2^2$. After solving this system subject to appropriate boundary conditions the four further variables $\bar{N}_1^1$, $\bar{M}_1^1$, $\bar{m}_3$ and $\dot{\bar{\delta}}_2$ can be determined immediately from equations (5.12) and (5.13). Note that $\dot{\bar{e}}_{22}$ can then be calculated using equation $(5.6)_2$ or the equation

$$\dot{\bar{e}}_{22} = -\dot{\bar{R}}_1 - \dot{\bar{\delta}}_3, \tag{5.19}$$

which is obtained by combining equations (5.6) and $(5.9)_1$ and which is the leading order form of the incompressibility condition.

For a homogeneous pipe, in which the parent and weld materials are identical, all z-dependence disappears from our problem. In this situation Hawkes [9] has shown that the simplified form of equations (5.15) to (5.18) yields stresses which agree to first order with the results of Bailey [14] (stated in a simpler form in Finnie and Haller [15]) for the creep of an internally pressurised, homogeneous, straight cylindrical pipe under plane strain conditions.

Asymptotic solution

Following the latter encouraging observation we now return to the system (5.15) to (5.18) for an inhomogeneous pipe and obtain an approximate solution as $\tau \to 0$ using matched asymptotic expansions (see Bender and Orszag [16] for details of the general method). Since it is the jump in $\bar{A}$ at the parent-weld interface $\bar{z} = 0$ which causes the deformation to vary with $\bar{z}$, we expect any boundary layer to appear near this interface.

Outer solution

To investigate the form of the solution at large distances from the interface it is necessary to introduce a transformed non-dimensional coordinate, z^*, and some transformed dependent variables. To obtain the correct leading order terms in the dependent variables it is found that the appropriate rescaled variables are

$$z^* = \tau^{-1/2}\bar{z}, \qquad N_{23}^* = \tau^{1/2}\bar{N}_{23}, \qquad M_{23}^* = \tau^{-1/2}\bar{M}_{23}, \tag{5.20}$$

$$M_{22}^* = \tau\bar{M}_2^2, \qquad \dot{\delta}_2^* = \tau^{1/2}\dot{\bar{\delta}}_2, \qquad \dot{S}^* = \tau^{1/2}\dot{\bar{S}}. \tag{5.21}$$

The leading order approximations in the asymptotic series representations for the dependent variables can now be found on using the expansions

$$\dot{S}^* \sim \dot{S}_0 + \tau^{1/2}\dot{S}_1, \qquad \dot{\bar{R}}_1 \sim \dot{R}_{10} + \tau^{1/2}\dot{R}_{11}, \tag{5.22}$$

$$\dot{\bar{\delta}}_3 \sim \dot{\delta}_{30} + \tau^{1/2}\dot{\delta}_{31}, \qquad M_{23}^* \sim M_{30} + \tau^{1/2}M_{31}, \tag{5.23}$$

$$N_{23}^* \sim N_{30} + \tau^{1/2}N_{31}, \qquad M_{22}^* \sim M_{20} + \tau^{1/2}M_{21}, \tag{5.24}$$

$$\dot{\delta}_2^* \sim \dot{\delta}_{20} + \tau^{1/2}\dot{\delta}_{21}, \tag{5.25}$$

in which all terms of $O(\tau)$ and higher are neglected.

On using (5.20) to (5.25) the system of equations (5.15) to (5.18) yields, on equating terms of $O(1)$,

$$\frac{d\dot{S}_0}{dz^*} = 18\bar{A}M_{20}, \qquad \frac{d\dot{R}_{10}}{dz^*} = -\dot{S}_0, \tag{5.26}$$

$$\frac{d\dot{\delta}_{30}}{dz^*} = 72\bar{A}M_{30}, \qquad 3\bar{A} + \dot{R}_{10} + 2\dot{\delta}_{30} = 0, \tag{5.27}$$

$$\frac{dN_{30}}{dz^*} = \frac{1}{3\bar{A}}(3\bar{A} + 2\dot{R}_{10} + \dot{\delta}_{30}) - \bar{p}_d, \qquad \frac{dM_{20}}{dz^*} = N_{30}, \tag{5.28}$$

and equation $(5.13)_2$ gives

$$\dot{\delta}_{20} = 6\bar{A}N_{30}. \tag{5.29}$$

After eliminating $\dot{\delta}_{30}$ with the use of equation $(5.27)_2$, the four equations (5.26) and (5.28) combine to produce the single fourth order differential equation

$$\frac{\mathrm{d}^4 \dot{R}_{10}}{\mathrm{d}z^{*4}} + 9\dot{R}_{10} = 9\bar{A}(2\bar{p}_d - 1), \tag{5.30}$$

with solution

$$\dot{R}_{10} = \sum_{i=1}^{4} C_i \, \mathrm{e}^{\lambda_i z^*} + \bar{A}(2\bar{p}_d - 1), \tag{5.31}$$

where C_i are constant and λ_i $(i = 1, \ldots, 4)$ are the four complex numbers satisfying $\lambda^4 + 9 = 0$. The corresponding solutions for $\dot{S}_0$, M_{20}, $\dot{\delta}_{30}$, M_{30} and N_{30} are easily calculated using the solution (5.31) together with equations (5.26), (5.27) and $(5.28)_1$.

Equation (5.30) is of identical form to that found using the classical theory of plates and shells (see Timoshenko [17]) for the radial displacement of an elastic cylindrical pipe of circular cross-section and constant thickness under symmetric loading. Within the classical theory the stress perpendicular to the reference surface is taken to be zero and there is no attempt to model the thinning of the pipe walls. The fact that (5.30) governs the outer solution shows that far away from the parent-weld interface the asymptotic solution as $\tau \to 0$ is dominated by the bending of the pipe's reference surface.

Inner solution

To determine the solution in the boundary layer close to the weld interface a new length scale must be introduced. The six continuity equations at the interface can be satisfied only if the system of equations remains of sixth order and to achieve this, with $\dot{\bar{\delta}}_3$ and $\bar{M}_{23}$ not identically constant, the necessary transformations are

$$\hat{z} = \tau^{-1/2} z^*, \qquad \hat{M}_{23} = \tau^{1/2} M^*_{23}. \tag{5.32}$$

Replacing $(5.23)_2$ by

$$\hat{M}_{23} \sim \hat{M}_{30} + \tau^{1/2} \hat{M}_{31}, \tag{5.33}$$

but leaving the remaining equations (5.22) to (5.25) unchanged, the leading equations now become

$$\frac{\mathrm{d}\dot{S}_0}{\mathrm{d}\hat{z}} = 0 = \frac{\mathrm{d}\dot{R}_{10}}{\mathrm{d}\hat{z}} = \frac{\mathrm{d}N_{30}}{\mathrm{d}\hat{z}} = \frac{\mathrm{d}M_{20}}{\mathrm{d}\hat{z}}, \tag{5.34}$$

$$\frac{\mathrm{d}\dot{\delta}_{30}}{\mathrm{d}\hat{z}} = 72\bar{A}\hat{M}_{30}, \qquad \frac{\mathrm{d}\hat{M}_{30}}{\mathrm{d}\hat{z}} = \frac{1}{3\bar{A}}(3\bar{A} + \dot{R}_{10} + 2\dot{\delta}_{30}). \tag{5.35}$$

It follows immediately from equations (5.34) that within the inner region

$$\dot{S}_0, \dot{R}_{10}, N_{30} \text{ and } M_{20} \text{ are all constant,} \tag{5.36}$$

and equations (5.35) then combine to produce a second order differential equation for $\dot{\delta}_{30}$ with

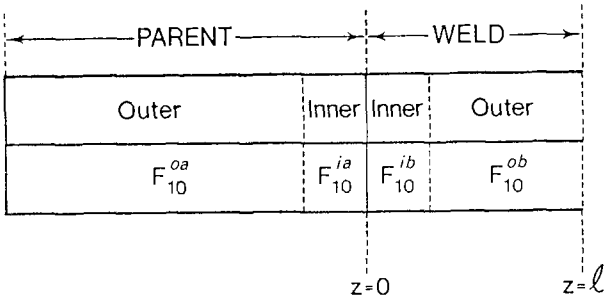

Fig. 2. Inner and outer regions (in diagrammatic form) for asymptotic solution, with the corresponding notation.

solution

$$\dot{\delta}_{30} = K_1 e^{-\sqrt{48}\hat{z}} + K_2 e^{\sqrt{48}\hat{z}} - \frac{3\bar{A}}{2} - \frac{\dot{R}_{10}}{2}, \tag{5.37}$$

where K_1 and K_2 are constants. The corresponding value of $\hat{M}_{30}$ is calculated using $(5.35)_1$.

Matching inner and outer solutions

As shown in Fig. 2 there exists an inner boundary layer, which surrounds the parent-weld interface $z = 0$, and two outer regions, one in $z < 0$ and the other in $z > 0$. Recalling $(5.5)_2$ it is assumed that $\bar{A} = 1$ and $\bar{A} = A_b$, a constant, in the parent material and weld respectively. Metallurgical examination suggests that this assumption of two distinct homogeneous regions is a good approximation. Since the inner region bridges the parent-weld interface, the inner solution must satisfy all the continuity conditions at $z = 0$, where $\bar{A}$ jumps from 1 to A_b. Let us attach superscripts o and i to all dependent variables in the outer and inner regions respectively and, further, use additional superscripts a and b for regions where $z < 0$ and $z > 0$ respectively.

In the outer region where $z < 0$ it follows immediately from $(5.27)_2$ and (5.31) that

$$\dot{R}_{10}^{oa} = \sum_{i=1}^{4} C_i^a e^{\lambda_i z^*} + 2\bar{p}_d - 1, \qquad \dot{\delta}_{30}^{oa} = -\frac{3}{2} - \frac{1}{2}\dot{R}_{10}^{oa}, \tag{5.38}$$

where

$$\lambda_1 = -\lambda_3 = (1.5)^{1/2}(1 + i), \qquad \lambda_2 = -\lambda_4 = (1.5)^{1/2}(1 - i). \tag{5.39}$$

Recalling the system of equations (5.26) to (5.28), the four stress components appearing in (4.23) remain finite as $z \to -\infty$ only if

$$C_3^a = 0 = C_4^a. \tag{5.40}$$

Analogous to (5.38) the outer solution in the region $z > 0$ is

$$\dot{R}_{10}^{ob} = \sum_{i=1}^{4} C_i^b e^{\lambda_i z^*} + A_b(2\bar{p}_d - 1), \qquad \dot{\delta}_{30}^{ob} = -\frac{3}{2}A_b - \frac{1}{2}\dot{R}_{10}^{ob}. \tag{5.41}$$

With the aid of equation (5.28) and the earlier transformation of variables, it is easily shown that conditions $(4.22)_{1,4}$ are equivalent to

$$\frac{\mathrm{d}\dot{R}_{10}^{ob}}{\mathrm{d}z^*} = 0 = \frac{\mathrm{d}^3\dot{R}_{10}^{ob}}{\mathrm{d}z^{*3}} \text{ on } z^* = l/(\tau^{1/2}R_0). \tag{5.42}$$

Substitution of $(5.41)_1$ into (5.42) then provides two equations linking the coefficients C_i^b.

Moving to the two inner regions it follows from the continuity requirements on the variables (4.19) and (4.20), with the aid of (5.14), (5.34) to (5.36) and the relevant transformations of variables, that $\dot{S}_0$, $\dot{R}_{10}$, N_{30} and M_{20} must all be continuous at $z = 0$, and hence that throughout both inner regions

$$\dot{S}_0^i = \dot{S}^c, \qquad \dot{R}_{10}^i = \dot{R}^c, \qquad N_{30}^i = N^c, \qquad M_{20}^i = M^c, \tag{5.43}$$

where $\dot{S}^c$, $\dot{R}^c$, N^c and M^c are constants. With the use of $(5.35)_1$ and (5.37), the remaining continuity conditions on M^{23} and $\dot{\delta}_3$ then yield

$$K_1^a + K_2^a - \frac{3}{2} = K_1^b + K_2^b - \frac{3}{2}A_b, \tag{5.44}$$

$$A_b(K_1^a - K_2^a) = K_1^b - K_2^b. \tag{5.45}$$

The ten additional equations required to allow determination of all the constants in the leading terms in our asymptotic solution are obtained from use of the matching principle. Since our inner and outer solutions are exponential the required matching is most easily obtained using

$$\lim_{\hat{z}\to-\infty}(F^{ia}) = \lim_{z^*\to 0-}(F^{oa}), \qquad \lim_{\hat{z}\to+\infty}(F^{ib}) = \lim_{z^*\to 0+}(F^{ob}), \tag{5.46}$$

where F denotes the variables $\dot{\delta}_{30}$, $\dot{S}_0$, $\dot{R}_{10}$, M_{20} and N_{30} in turn. With the aid of (5.26), $(5.28)_2$, (5.38), (5.40), (5.41) and (5.43) conditions (5.46) lead to

$$K_1^a = 0 = K_2^b, \qquad \sum_{i=1}^{2} C_i^a\lambda_i = -\dot{S}_c = \sum_{i=1}^{4} C_i^b\lambda_i, \tag{5.47}$$

$$\sum_{i=1}^{2} C_i^a + 2\bar{p}_d - 1 = \dot{R}_c = \sum_{i=1}^{4} C_i^b + A_b(2\bar{p}_d - 1), \tag{5.48}$$

$$\sum_{i=1}^{2} C_i^a\lambda_i^2 = -18M^c = A_b^{-1}\sum_{i=1}^{4} C_i^b\lambda_i^2, \tag{5.49}$$

$$\sum_{i=1}^{2} C_i^a\lambda_i^3 = -18N^c = A_b^{-1}\sum_{i=1}^{4} C_i^b\lambda_i^3. \tag{5.50}$$

All the constants can now be determined.

In terms of the outer length scale z^* the composite solution can be expressed

$$\dot{R}_{10} = \begin{cases} \displaystyle\sum_{i=1}^{2} C_i^a e^{\lambda_i z^*} + 2\bar{p}_d - 1, & z^* \leqslant 0 \\ \displaystyle\sum_{i=1}^{4} C_i^b e^{\lambda_i z^*} + A_b(2\bar{p}_d - 1), & 0 \leqslant z^* \leqslant l^* \end{cases} \tag{5.51}$$

$$\dot{\delta}_{30} = \begin{cases} \dfrac{3(1-A_b)}{2(1+A_b)} e^{\sqrt{48}\tau^{-1/2}z^*} - \dfrac{1}{2}\dot{R}_{10} - \dfrac{3}{2}, & z^* \leqslant 0 \\ \dfrac{3A_b(A_b-1)}{2(1+A_b)} e^{-\sqrt{48}\tau^{-1/2}z^*} - \dfrac{1}{2}\dot{R}_{10} - \dfrac{3}{2}A_b, & 0 \leqslant z^* \leqslant l^* \end{cases} \tag{5.52}$$

where $l^* = l/(\tau^{1/2}R_0)$. Equation (5.51) shows that when z^* is O(1) (i.e. $z = \mathrm{O}(hR_0)^{1/2}$) $\dot{R}_{10}$ is largely determined by the bending solution, whereas when z^* is $\mathrm{O}(\tau^{1/2})$ (i.e. $z = \mathrm{O}(h)$) $\dot{R}_{10}$ is approximately constant and no bending is observed. In an analogous way (5.52) reveals that the rate of thinning $\dot{\delta}_{30}$ is determined by the solution $\dot{R}_{10}$ when z^* is O(1), but is similar to the flat plate solution when z^* is $\mathrm{O}(\tau^{1/2})$. The result that bending and thinning occur on different length scales is assumed by Taheri [18] in his calculations of creep strain rate.

Analytical solution

The governing system (5.15) to (5.18) can be written in the matrix form

$$X' = LX + B, \tag{5.53}$$

where a prime denotes differentiation with respect to $\bar{z}$,

$$X^T = [\bar{M}_2^2,\ \bar{M}_{23},\ \bar{N}_{23},\ \dot{\bar{S}}/\bar{A},\ \dot{\bar{R}}_1/\bar{A},\ \dot{\bar{\delta}}_3/\bar{A}], \tag{5.54}$$

$$L = \begin{bmatrix} 0 & 0 & \tau^{-1} & 0 & 0 & 0 \\ 0 & 0 & 0 & 0 & (3\tau)^{-1} & 2(3\tau)^{-1} \\ 0 & 0 & 0 & 0 & 2(3\tau)^{-1} & (3\tau)^{-1} \\ 18 & 0 & 0 & 0 & -6^{-1} & 6^{-1} \\ 0 & -6\tau & 6\tau & -1 & 0 & 0 \\ 0 & 72\tau^{-1} & 0 & 0 & 0 & 0 \end{bmatrix} \tag{5.55}$$

$$B^T = \left[0, \tau^{-1} + \frac{1}{2}\bar{p}_s - \frac{1}{6}\bar{p}_d\tau, \tau^{-1} + \frac{1}{2}\bar{p}_s - \bar{p}_d\tau^{-1}, -\frac{3}{2}, 0, 0\right], \tag{5.56}$$

and to conclude this section this system is solved explicitly. The general solution to (5.53) is

$$X = \sum_{i=1}^{6} \alpha_i C_i e^{\mu_i \bar{z}} + X_c, \tag{5.57}$$

where the μ_i are the roots of the sextic equation

$$\mu^6 - (48\tau^{-2} + 13/6)\mu^4 + 168\mu^2\tau^{-2} - 432\tau^{-4} = 0, \tag{5.58}$$

C_i are the eigenvectors corresponding to each μ_i and

$$X_c^T = -(L^{-1}B)^T = \left[\frac{1}{12} + \frac{\bar{p}_d}{36}, 0, 0, 0, -1 + 2\bar{p}_d - \frac{1}{2}\bar{p}_s\tau, -1 - \bar{p}_d - \frac{1}{2}\bar{p}_s\tau\right]. \tag{5.59}$$

The constants α_i, which equal α_i^a and α_i^b in the parent and weld regions respectively, are determined by applying the conditions

$$\frac{\mathrm{d}\bar{M}_2^2}{\mathrm{d}\bar{z}} = 0 = \bar{N}_{23} \text{ as } \bar{z} \to -\infty, \tag{5.60}$$

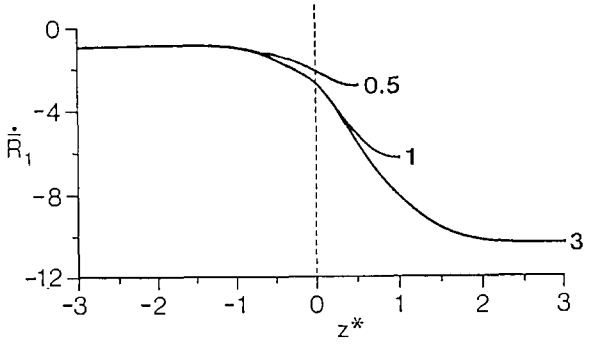

Fig. 3. Plots of $\dot{\bar{R}}_1$ against z^* $(= \tau^{1/2} z/h)$, for stated values of the weld width l^*, when $\tau = 0.1$, $A_b = 10$, $p_s = p_d = 0$.

$$\bar{M}_2^2,\ \bar{N}_{23},\ \bar{M}_{23},\ \dot{\bar{R}}_1,\ \dot{\bar{S}},\ \dot{\bar{\delta}}_3 \text{ continuous at } \bar{z} = 0, \tag{5.61}$$

$$\bar{N}_{23} = 0 = \bar{M}_{23} = \dot{\bar{S}} \text{ at } \bar{z} = l/R_0. \tag{5.62}$$

A solution to the system (5.15) to (5.18) can thus be found directly, but some of the important qualitative features of this solution are not obvious from the form of expression (5.57).

6. Results

The detailed analysis in Section 5 enables us to calculate both the analytical and asymptotic solutions for the special case $n = 1$. Figure 3 shows the analytical solution for $\dot{\bar{R}}_1$, the non dimensional rate of change of radius of the reference surface, in a thin pipe ($\tau = 0.1$) containing a soft weld ($A_b = 10$), under uniaxial tension with no applied pressures ($p_s = p_d = 0$), plotted against the outer length scale for a variety of weld widths ($l^* = 1/2$, 1 and 3, approximately equivalent, in dimensional variables, to $l = 1.6$h, 3.2h and 9.5h). Figure 3 confirms that the pipe bends over a long length scale, a result which is consistent with classical plate theory. It is also evident from Fig. 3 that the value of $\dot{\bar{R}}_1$ on the reference surface is negative everywhere (i.e. the radius of the pipe's reference decreases with time) and that the magnitude of the strain rate in the soft weld region is greater than its value in the much stronger parent material. When the width of the weld decreases Fig. 3 reveals that the maximum magnitude of the strain rate at the centre of the weld also decreases. Results qualitatively similar to those shown in Fig. 3 are obtained when the thickness of the pipe walls is reduced, but all other parameters are unchanged.

It is important to note that for the particular values of the parameters leading to Fig. 3 the maximum percentage difference in $\dot{\bar{R}}_1$ between its analytical and asymptotic values is about 5% of its asymptotic value, and this maximum occurs close to the parent-weld interface. Not unexpectedly the percentage difference decreases when the ratios A_b and τ decrease.

Plots of $\dot{\bar{\delta}}_3$ against distance are shown in Fig. 4 with, again, $\tau = 0.1$, $A_b = 10$ and $p_s = p_d = 0$. It is important to note that distance in Fig. 4 is the inner length scale $\hat{z}$ $(= z/h)$ whereas Fig. 3 uses the outer length scale z^* $(= \tau^{1/2} z/h)$. The variable $\dot{\bar{\delta}}_3$ is related to the rate of thinning of the pipe walls. Figure 4 clearly shows that the thinning rate changes from its constant value in the parent material to the different constant value in the weld zone within

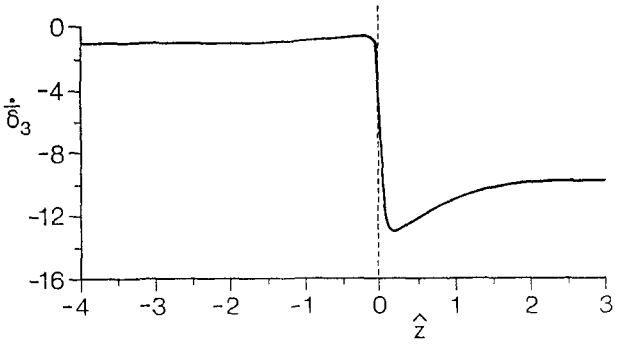

Fig. 4. Plots of $\dot{\bar{\delta}}_3$ against $\hat{z}$ $(= z/h)$ when $l = 3h$, $\tau = 0.1$, $A_b = 10$, $p_s = p_d = 0$.

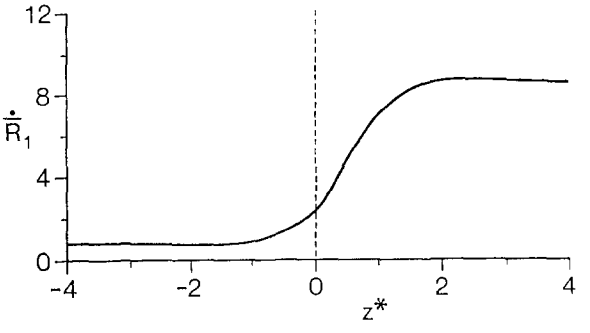

Fig. 5. Plots of $\dot{\bar{R}}_1$ against z^* $(= \tau^{1/2} z/h)$, when $l^* = 4$, $\tau = 0.1$, $A_b = 10$, $p_s = 3$, $p_d = 1$.

a relatively narrow region close to the interface. This region has approximate width h, which is the same length scale that governs the thinning of a plate.

Hawkes [9] has calculated results, analogous to those discussed above, for a wide hard weld $(A_b = 0.1)$ in a non-pressurised pipe under uniaxial tension. As expected the strain rates now have their maximum magnitudes in the parent material. Hawkes' results and the ones shown in Fig. 4 demonstrate, not surprisingly, that the most thinning of the pipe walls occurs in the softer material, wherever that material lies.

Finally, two sets of results are presented for pipes subjected to internal and external pressures, in addition to tensile loading. For the choice $p_i = 2.0$ and $p_e = 1.0$ (i.e. $p_d = 1.0$

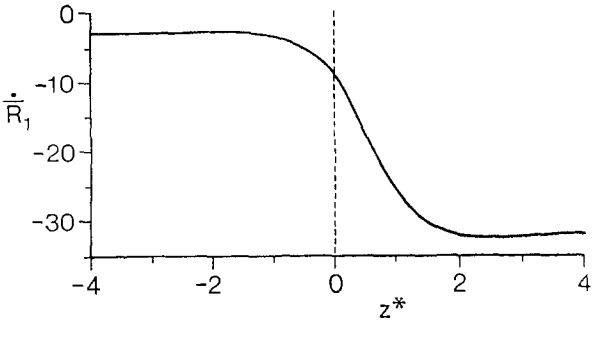

Fig. 6. Plots of $\dot{\bar{R}}_1$ against z^* $(= \tau^{1/2} z/h)$, when $l^* = 4$, $\tau = 0.1$, $A_b = 10$, $p_s = 3$, $p_d = -1$.

and $p_s = 3.0$), but all other parameters as for Fig. 3, the strain rate $\dot{\bar{R}}_1$ on the reference surface is plotted against z^* in Fig. 5. Observe that in this case the strain rate is everywhere positive and so the radius of the reference surface increases with time.

When the internal and external pressures are changed to $p_i = 1.0$ and $p_e = 2.0$ (i.e. $p_d = -1.0$ and $p_s = 3.0$) the resulting strain rate on the reference surface is shown in Fig. 6. In this situation the strain rate is negative and hence the radius of the reference surface decreases with time.

One important, though unfortunate, feature of Figs. 3 to 6 is the appearance of a small oscillation about the expected form of solution. In Fig. 4, for instance, the magnitude of $\dot{\bar{\delta}}_3$ in the parent material decreases from its uniform value as the interface is approached and then, after a rapid change near $\hat{z} = 0$, overshoots its uniform value at the centre of the weld region. This oscillation is due to the presence of complex roots for λ_i in the asymptotic solution (5.51) or, equivalently, the appearance of complex roots μ_i in the analytical solution (5.57). Fortunately, the effect of these complex roots on the overall form of solution is small and the oscillation is expected to become less evident as n increases.

7. Conclusion

With the use of a Cosserat model which includes a single director both asymptotic and analytical solutions have been obtained in this paper for a thin pipe under constant tensile end loading and optional pressure loading. The pipe may inflate or narrow in time depending on the relative magnitudes of the applied pressures and tensile force. The asymptotic results have shown that for a thin walled pipe the thinning of the pipe walls occurs over a much shorter length scale than that associated with the bending of the pipe. Moreover, the first term in the asymptotic series has been shown to yield results which are very close to the exact solution of the system of differential equations obtained with our model.

Results have been obtained in this paper for thin walled pipes in which the materials satisfy a generalised Norton's law with creep index equal to unity. Extension of this model to more realistic values of the creep index is expected to be straightforward.

References

1. I. W. Goodall and D. J. Walters, Creep behaviour of butt-welded tubes. *Inst. Mech. Engineers Conf. publication* 13 (1973).
2. D. J. Walters, The stress analysis of cylindrical pipe welds under creep conditions. CEGB report RD/B/M3716 (1976).
3. M. C. Colman, J. D. Parker and D. J. Walters, The behaviour of ferritic weldments in thick section 1/2CrMoV pipe at elevated temperatures. CEGB report RD/M/1204/R81 (1981).
4. F. R. Hall and D. R. Hayhurst, Continuum damage mechanics modelling of high temperature deformation and failure in a pipe weldment. *Proc. R. Soc. Lond.* 433 (1991) 383–403.
5. S-T. Tu and R. Sandström, Numerical simulation of creep exhaustion of weldments and some design considerations. In B. Wilshire and R. W. Evans (eds.), Creep and fracture of engineering materials and structures, Proc. of 5th Int. Conf. The Institute of Materials, London (1993) 695–704.
6. D. A. C. Nicol, Creep behaviour of butt-welded joints. *Int. J. Engng Sci.* 23 (1985) 541–553.
7. P. M. Naghdi, *The theory of shells and plates*. In: C. Truesdell (ed.), Handbuch der Physik, vol. VIa/2 (1972), reissued as Mechanics of Solids, vol. II (1984) Springer-Verlag, Berlin.
8. D. A. C. Nicol and J. A. Williams, The creep behaviour of cross-weld specimens under uniaxial loading. *Res. Mechanica* 14 (1985) 197–223.
9. T. D. Hawkes, *Mathematical modelling of the creep of weldments using the Cosserat theory of plates and shells*. Ph.D. Thesis. University of Southampton (1989).
10. R. E. Craine and T. D. Hawkes, On the creep of ferritic weldments containing multiple zones in plates under uniaxial loading. *J. Strain Anal. and Engng Design* 28 (1993) 303–309.

11. M. G. Newman and R. E. Craine, Creep failure in thin plates. In A. C. F. Cocks and A. R. S. Ponter (eds.), Mechanics of creep brittle materials – 2, pp. 296–307. Elsevier Applied Science, (1991).
12. M. G. Newman and R. E. Craine, Modelling type IV cracking in thin plates under uniaxial loading. In S. I. Andersen, J. B. Bilde-Sorensen, N. Hansen, D. Juul Jensen, T. Leffers, H. Lilholt, T. Lorentzen, O. B. Pedersen and B. Ralph (eds.), Modelling of Plastic Deformation and Its Engineering Applications, Proc. of 13th Int. Symp. on Materials Science, pp. 241–246. Riso National Laboratory, Roskilde, Denmark (1992).
13. M. G. Newman, *Mathematical modelling of creep in weldments using the Cosserat theory of plates and shells*. Ph.D. Thesis. University of Southampton (1993).
14. R. W. Bailey, Creep relationships and their application to pipes, tubes and cylindrical parts under internal pressure. Proc. Inst. Mech. Engrs 164 (1951) 425–431.
15. I. Finnie and W. R. Heller, Creep of Engineering Materials. McGraw-Hill, (1959).
16. C. M. Bender and S. A. Orszag, *Advanced Mathematical Methods for Scientists and Engineers*. McGraw-Hill, New York (1978).
17. S. Timoshenko, *Theory of plates and shells*. McGraw-Hill, New York (1940).
18. S. Taheri, Local effects due to discontinuous material property and discontinuous loading conditions. Presented at XVIIth Int. Congress of Theor. and Appl. Mech., Grenoble (1988).